Supplementary Information(SI)

Stepped M@Pt(211) (M = Co, Fe, Mo) single-atom alloys promote deoxygenation of lignin-derived phenolics: mechanism, kinetics and descriptor

Ranran Liu, Wei An*

College of Chemistry and Chemical Engineering, Shanghai University of Engineering Science, 333 Longteng Road, Songjiang District, Shanghai 201620, China

*E-mail: weian@sues.edu.cn

S1. Adsorption/desorption, zero-point energy (*ZPE*) and entropy corrections (*TS*)

The adsorption of phenol (**R1**) and the dissociative adsorption of H_2 (**R2**) are assumed to follow Langmuir adsorption mode and in thermodynamics equilibriums. As such, we can estimate the adsorption constant based on the calculated adsorption energies and the estimated entropy changes from gas phase to the adsorbed species by approximating the change as condensation. Thus, the equilibrium constant was estimated based on $K = \exp[-(\Delta E_{ads} - T\Delta S)/k_B T]$, where ΔE_{ads} is *ZPE*-corrected adsorption energy of phenol or *ZPE*-corrected reaction energy of H_2 dissociation on M@Pt(211), and ΔS is the entropy change of adsorbed and gas-phase phenol or H_2, The entropy changes for gas-phase H_2, phenol, and benzene were obtained from NIST Chemistry WebBook:[1]

$$\Delta S(0 \to T, P^{\circ}) = \Delta S_{\text{ads}}(0 \to T, P^{\circ}) - \Delta S_{\text{gas}}(0 \to T, P^{\circ}) \qquad (1)$$

The entropy changes for adsorbed gas-phase were calculated using the harmonic approximation according to:

$$\Delta S_{ads}(0 \to T, P^{0}) = S_{vib} = \sum_{i=1}^{3N}\left[\frac{N_{\text{A}} h\nu_i}{T(e^{h\nu_i/k_B T} - 1)} - R\ln(1 - e^{-h\nu_i/k_B T})\right] \qquad (2)$$

where ν_{i} is the normal-mode frequency for species of 3N degree of freedom (N=number of atoms) adsorbed on Pt(211) or Mo@Pt(211).

S2. Microkinetic simulations

For the surface reactions, the rate constants for the forward and backward elementary reaction were determined by the Eyring equation:

$$k_n = A\exp(-E^0_{a,n} / k_B T) \qquad (3)$$

$$A = \frac{k_B T}{h}\frac{Q_{TS}}{Q_{IS}} \qquad (4)$$

where k_{n} is the reaction rate constant in s^{-1} and A is pre-exponential factor in s^{-1}, $E^0_{\text{a,n}}$ is activation barrier, T is reaction temperature, k_B and h are Boltzmann constant and Planck's constant, respectively. The zero-point energy (*ZPE*) corrections were included in the calculations of activation and reaction

energies. The vibrational partition functions of the transition and initial states, Q_{TS} and Q_{IS}, can be evaluated using the calculated harmonic frequencies based on:

$$Q_{vib} = \prod_i \frac{1}{1 - e^{-h\nu_i / k_B T}} \qquad (5)$$

where i runs to $3N$-1 and $3N$ for the transition state and initial state, respectively, N is the number of atoms for adsorbates.

Steady-state coverages for all reaction intermediates (listed in **Table 1)** were calculated by integrating the ordinary differential equations (ODEs) in time until the changes in the surface coverages were very small. The backward differentiation formula method for the time integration was implemented in MKMCXX[2] for solving the stiff sets of ODEs. The rates of the individual elementary reaction steps (r_n in site^{-1} s^{-1}) were obtained based on the computed steady-state surface coverages.

The input parameters including molecular mass (in amu), the adsorption/desorption equilibrium constant (K), activation free energy ($\Delta G^{0\neq}$, in joule/mole), reaction temperature (T, in Kelvin degree), pressure (P, in bar), and C_6H_5OH/H_2 molar ratio were entered for running MKMCXX. The output results include coverage, the reaction rate constant (k_n^+ and k_n^-, in s^{-1}) and reaction rate (r_n, site^{-1} s^{-1}).

Table S1. DFT-calculated surface segregation energy, OH-induced segregation energy, magnetic moment and Bader charge transfer of M@Pt(211) surface alloy, as shown in Figure S1.

M@Pt(211)	Co	Fe	Mo
E_{segr} (eV)	0.51	0.55	1.48
OH-E_{segr} (eV)[a]	−0.60	−0.84	−1.13
μ (μ_B)[b]	4.51	4.96	0.00
$\Delta\mu$ (μ_B)[c]	−0.06	−0.10	0.00
$M^{\Delta q+}$ (e^-)[d]	0.54	0.75	1.11
OH–$M^{\Delta q+}$ (e^-)	0.98	1.22	1.65
$OH^{\Delta q-}$ (e^-)[e]	0.40 (0.15)	0.42 (0.16)	0.56 (0.18)

[a]with full coverage of OH* at M site.

[b]μ: magnetic moment with M@Pt(211).

[c]$\Delta\mu$: decrease in magnetic moment due to adsorption of phenol.

[d]$M^{\Delta q+}$: electron charge transfer from M to host Pt atoms (Δq) resulting in partially oxidized $M^{\Delta q+}$.

[e]$OH^{\Delta q-}$: mean electron charge transfer from M and Pt to *OH (Δq) resulting in partially negatively charged $*OH^{\Delta q-}$, where the contribution from M is listed in parenthesis.

Table S2. DFT-calculated binding energy (*BE*) for surface species of *H, *OH, $*H_2O$, $*C_6H_6$, $*C_6H_5OH$ and $*C_6H_5OCH_3$ adsorbed on M@Pt(211) and Pt(211), where M = Co, Fe, Mo.

BE(eV)		Pt(211)	M@Pt(211)		
			Co	Fe	Mo
H[a]		−0.35	−0.33	−0.33	−0.32
OH[b]		−2.96	−3.00	−3.10	−3.51
H_2O		−0.42	−0.71	−0.74	−1.20
Benzene[c]		−2.01	−2.01	−1.99	−1.97
Phenol[c]	Vertical	−0.56	−1.00	−1.09	−1.48
	Parallel-(I)	−0.96	−0.96	−0.97	−1.35
	Parallel-(II)	−0.96	−0.71	−0.70	−1.27
	Parallel-(III)	−2.01	−1.97	−1.96	−1.99
Anisole[c]	Vertical	−0.95	−1.16	−1.20	−1.77
	Parallel	−1.53	−1.44	−1.49	−1.77

[a] $BE(H) = E(H/slab) - E(slab) - 0.5E(H_2)$.

[b] $BE(OH) = E(OH/slab) - E(slab) - E(OH)$.

[c] Calculated using optB88-vdW functional.

Table S3. Standard Gibbs free energy (ΔG^0_{rxn}), activation energy ($\Delta G^{0\neq}$), pre-exponential factor (A), forward rate constant (k^+) and backward rate constant (k^-) for each elementary step in the reaction mechanisms under the experimental conditions. (1/9 bar phenol, 1.0 bar H_2, and 573 K)

(a)

Pt(211)	ΔG^0_{rxn} (eV)	$\Delta G^{0\neq}$ (eV)	A^+ (s^{-1})	A^- (s^{-1})	k^+ (s^{-1})	k^- (s^{-1})
R3	1.90	2.07	2.3×10^{13}	4.2×10^{13}	3.9×10^{-5}	1.5×10^{5}
R4	–1.65	0.76	1.3×10^{13}	4.2×10^{12}	2.6×10^{6}	1.4×10^{-2}
R5	0.10	0.33	4.5×10^{13}	1.5×10^{15}	5.7×10^{10}	2.1×10^{13}
R6	–0.72	1.38	5.3×10^{14}	3.7×10^{13}	9.3×10^{12}	1.2×10^{-10}
R7	-0.12	0.53	2.3×10^{13}	5.9×10^{12}	5.1×10^{8}	2.4×10^{8}

(b)

Mo@Pt(211)	ΔG^0_{rxn} (eV)	$\Delta G^{0\neq}$(eV)	A^+ (s^{-1})	A^- (s^{-1})	k^+ (s^{-1})	k^- (s^{-1})
R3	0.14	0.50	1.6×10^{14}	1.6×10^{13}	9.0×10^{2}	1.5×10^{3}
R4	–1.05	0.72	3.2×10^{13}	1.9×10^{13}	1.8×10^{7}	1.4×10^{-1}
R5	0.12	0.31	5.5×10^{12}	7.8×10^{13}	1.0×10^{10}	4.6×10^{12}
R6	–2.16	0.36	8.6×10^{13}	4.7×10^{12}	9.3×10^{12}	1.2×10^{-10}
R7	0.49	0.76	4.2×10^{13}	4.0×10^{13}	1.4×10^{6}	2.7×10^{10}

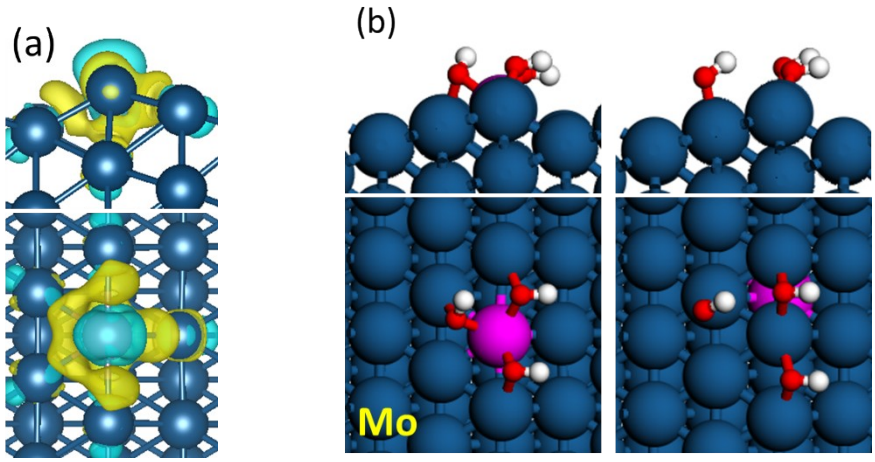

Figure S1. (a) The charge-density difference ($\Delta\rho$) of Mo@Pt(211). Isosurface level: 0.004 e/bohr^3; yellow: charge accumulation; cyan: charge depletion. (b) Configurations of three *OH adsorbed at bridge site of Pt-Mo on surface alloy (SA) and near-surface alloy (NSA) for calculating *OH-induced surface segregation energy (E_{segr}) shown in Figure 1a.

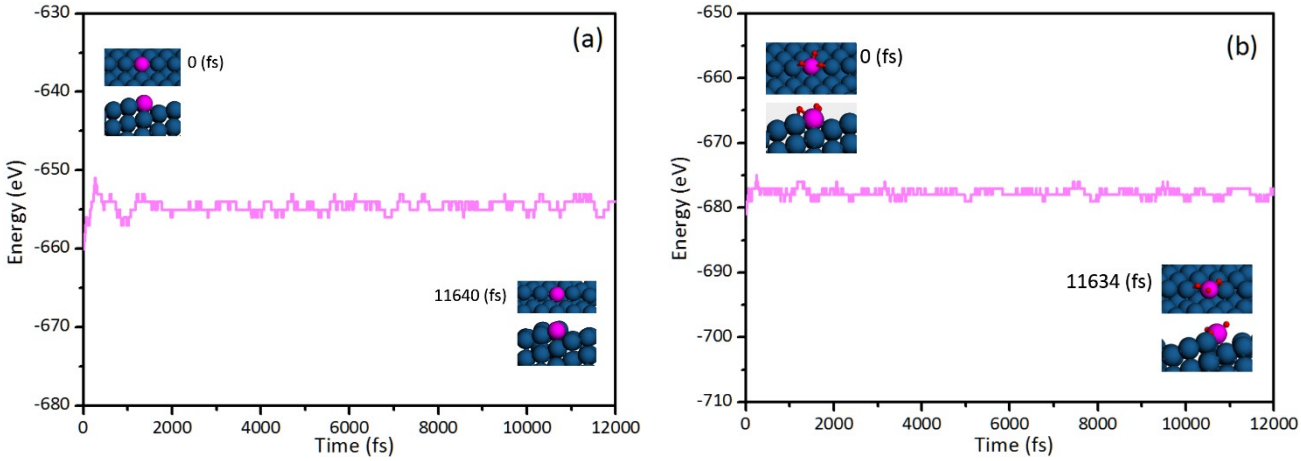

Figure S2. (a) Mo@Pt(211) and (b) three O atoms adsorbed on Mo@Pt(211) in AIMD simulations at 673 K. The snapshots of local-minimum structures were displayed.

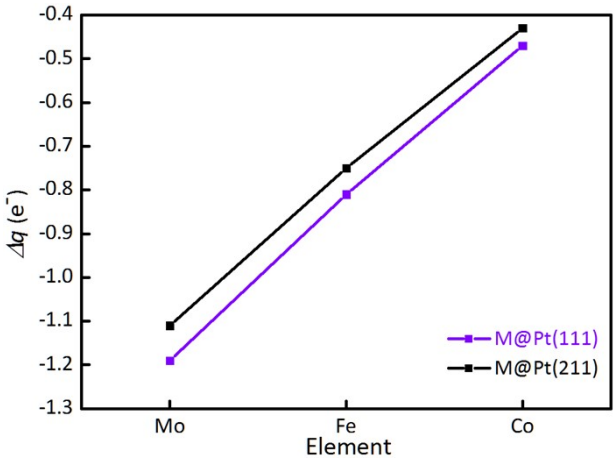

Figure S3. Variation of electron charge (Δq, per M atom) transferred from alloyed M to host Pt in M@Pt(211) and M@Pt(111)[3].

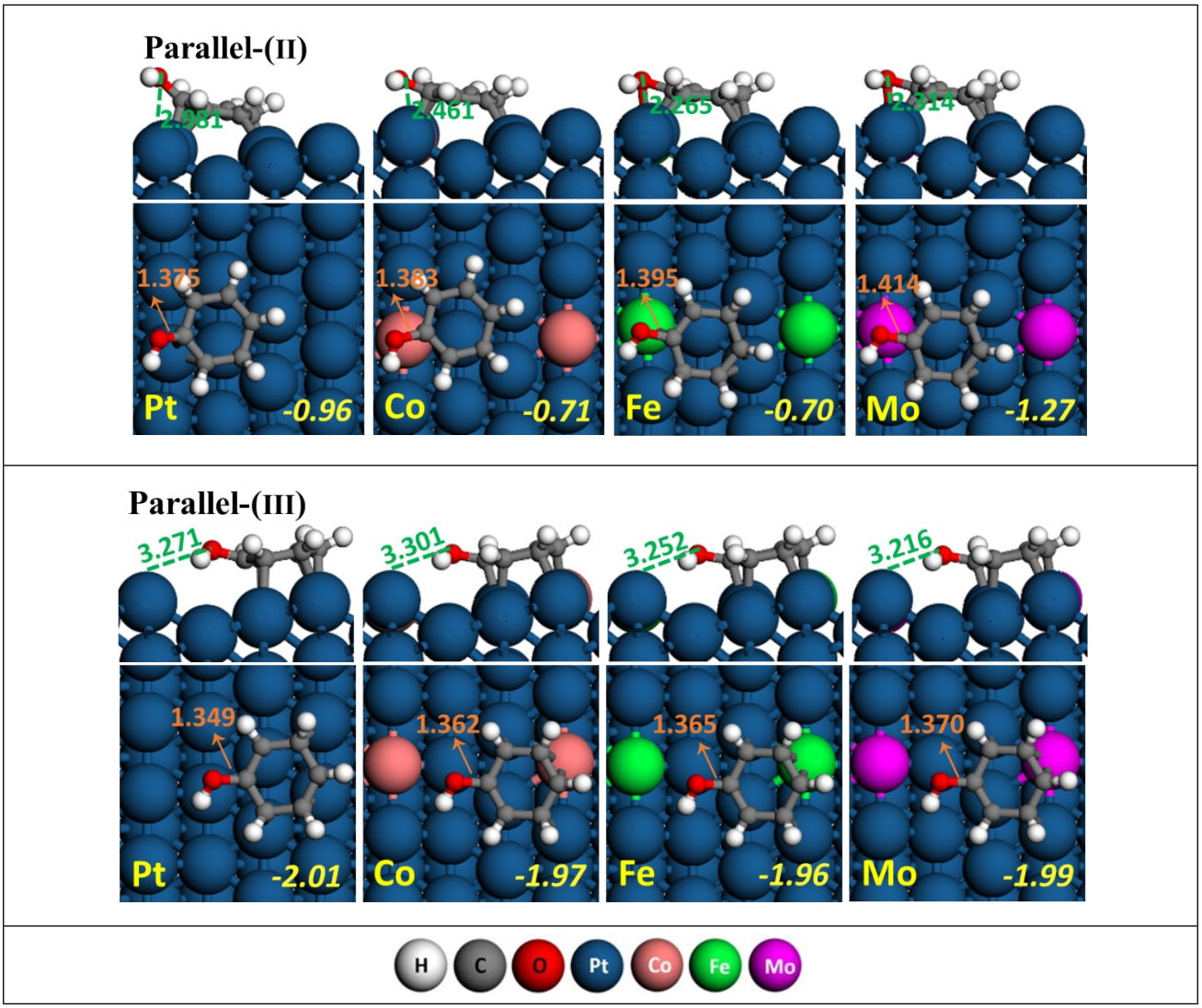

Figure S4. Optimized configurations of phenol parallel adsorption on M@Pt(211). Regular numeric: C−OH bond length (in Å); Italic numeric: binding energy (in eV) calculated using optB88-vdW functional.

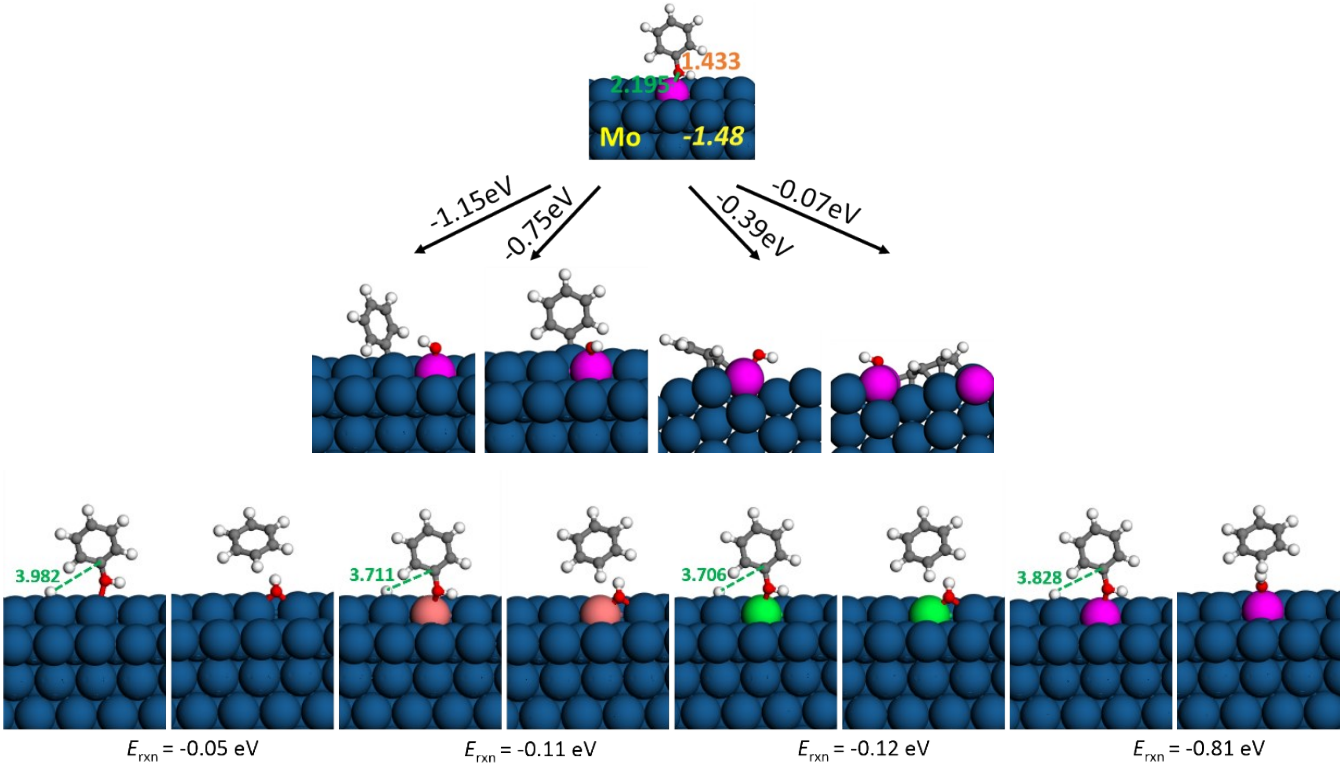

Figure S5. Optimized initial state (IS) and final state (FS) configurations of the elementary steps (*C_6H_5OH + * → *C_6H_5 + *OH and *C_6H_6OH + * → *C_6H_6 + *OH) along phenol DDO and PHDO pathways. The reaction energy (E_{rxn}, eV) are displayed.

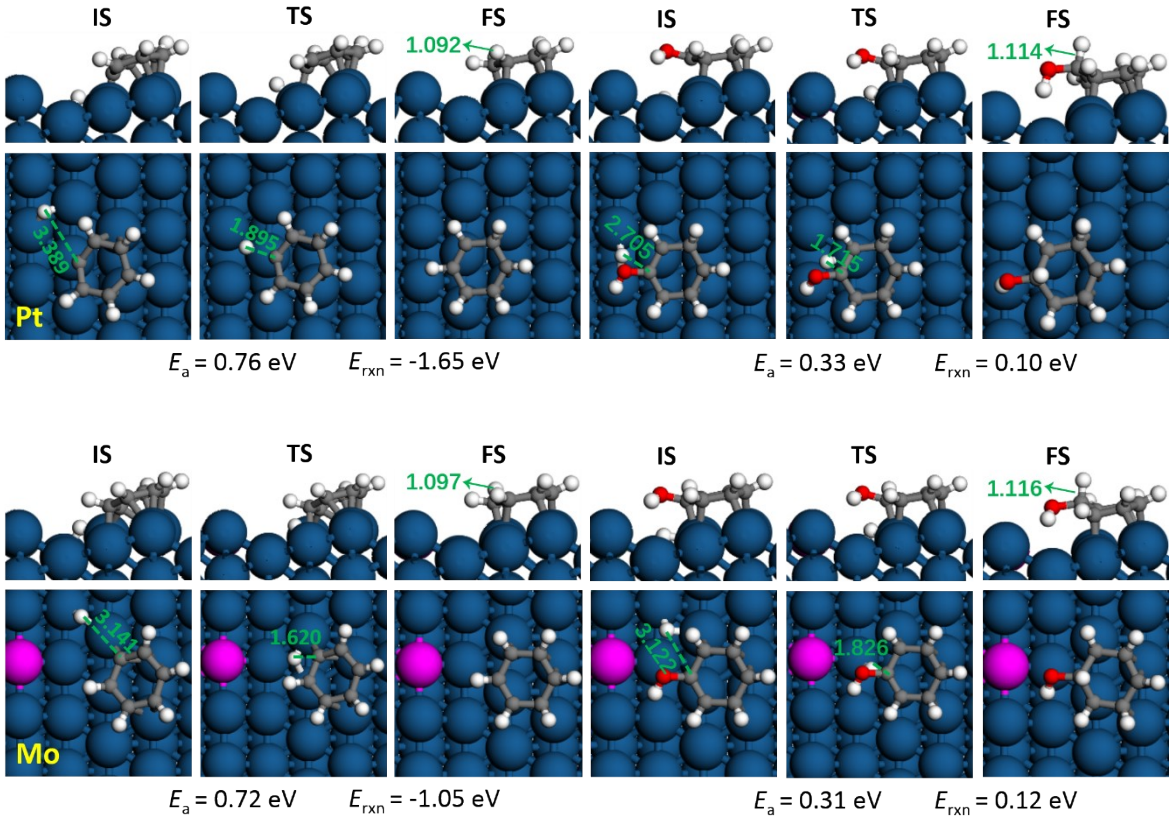

Figure S6. Optimized initial state (IS), transition state (TS) and final state (FS) configurations of the hydrogenation steps ($*C_6H_5 + *H \rightarrow *C_6H_6 + *$ and $*C_6H_5OH + *H \rightarrow *C_6H_6OH + *$) along DDO and PHDO reaction pathways on Pt(211) and Mo@Pt(211). The C–H bond length (Å), activation energy (E_a, eV) and reaction energy (E_{rxn}, eV) are displayed.

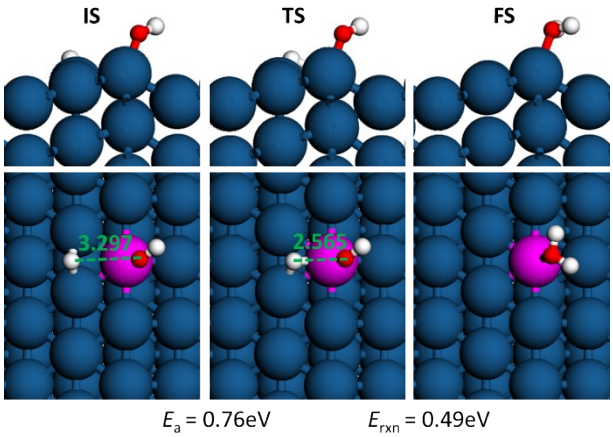

Figure S7. Optimized initial state (IS), transition state (TS) and final state (FS) configurations of the formation of H_2O.

References

1 http://webbook.nist.gov/chemistry/.

2 I. A. W. Z. Filot, B.; Hensen, E. J. M. http://www.mkmcxx.nl.

3 X. Jia, W. An, Z. Wang and J. Zhou, Effect of doped metals on hydrodeoxygenation of phenol over Pt-based bimetallic alloys: C_{aryl}-OH versus $C_{aliphatic}$H-OH bond scission, *J. Phys. Chem. C*, 2019, **123**, 16873-16882.